



Animated View for Detection of Hairline Fracture of the Cooling Hole of a Tornado Jet Turbine Blade by a CAD Based on the De-Convolution Technique

Kui-Ming CHUI¹, Shu-Yan ZHANG², Eberhard LEHMANN³, Anders KAESTNER⁴,
Shyr-Lin CHUI⁵, David STANFIELD¹, Andrew WRIDE¹

¹ Image Enhancement Technology Ltd., Uxbridge, UK

² Science and Technology Facilities Council, Didcot, Oxfordshire, UK

³ PSI - Paul Scherrer Institut, Switzerland

⁴ PSI - Paul Scherrer Institut, Villigen PSA, Switzerland

⁵ University Hospital of Northern British Columbia, Prince George, BC, Canada

Contact e-mail: ming-chui@iet.org.uk

Abstract. Blurred image edges caused by the Penumbra Effect have existed since the discovery of X-rays. In Computed Tomography (X-ray or Neutron-Beam), the combined effect of the size(s) of the energy source and the detector(s) cause the Penumbra Spread. Recently, by using the processing power of modern CPUs, we have found a software solution to the problem - a post-processing De-Convolution Technique for the detection, definition, and enhancement of image edge profiles. Enhancement is carried out in a zoomed space within which, the higher the magnification factor, the clearer the enhanced image, as both the Penumbra and the Pixelization Effects are overcome simultaneously. The overall effect is to re-focus the image edge-profile, as if derived from an infinitely small energy source. This patented technique has all the advantages of sensitivity, sub-pixel accuracy, and efficiency (in terms of processing-time). By solving this previously 'unsolvable' problem, numerous important applications may now be realized.



1. Introduction

1.1. Object or Purpose of Study

The Penumbra Effect describes blurring at the margins of an image profile due to the finite size of the energy source. A computer aided detection (CAD) algorithm based on the De-Convolution Technique can be used to pinpoint true edge positions to sub-pixel accuracy and remove the Penumbra Effect (and at the same time, the removal of the Pixelization Effect) via sub-pixel transfers without trade-off losses [1]. Derived from this, a definitive method of accurate measurement may have been found. 50 slices of NBCT images on four cooling holes of a used jet turbine blade were analyzed to search for the 'invisible' hairline fracture.

2. Specific Experimental Details

2.1. Materials, Methods, and Procedures

2.1.1. Phantoms

Composite phantom and New-York Catphan-500 were used to provide X-ray CT images to verify the accuracies of the De-Convolution Technique [1].

2.1.2. Neutron-Beam Computed Tomography (NBCT):

The neutron-beam imaging experiment was performed at the cold neutron imaging beamline ICON of the SINQ spallation neutron source at the Paul Scherrer Institut (PSI) [2]. The neutrons at the beamline originate from the cold moderator of the SINQ (25K) and have an energy spectrum with peak at 25meV and an average energy of 8.5meV. Using the high-resolution imaging setup at experimental position 2 and a neutron aperture of 20mm the collimation ratio was $L/D=340$. This was sufficient to assume parallel beam geometry for the given sample size. The pixel size was 13.5 microns and the resolution 21 Lp/mm. The CT projection data consisted of 625 projections (2048x2048 pixels) on a 360 degree scan. The projection data was reconstructed using a filtered back-projection algorithm for parallel beam.

2.2. Results

2.2.1. Phantom Calibration by X-ray CT

Measurements: Distance – at high-contrast and 1% low-contrast edge, both accurate to $1/50^{\text{th}}$ of a pixel. Area/Volume - at high-contrast and 1% low-contrast edge, accurate to $1/18^{\text{th}}$ and $1/10^{\text{th}}$ of a pixel respectively.

2.2.2. NBCT images

505 Neutron-Beam CT image slices through a jet turbine blade, end to end, (0.0132mm/slice) were collected by Cone Beam Geometry CT.

2.2.3. Field Examples

A used Tornado jet engine turbine blade (C3FOX) was analyzed. To cover the complete blade, 505 slices of thickness 0.0132mm/slice were obtained. 50 slices starting from #0520, #0530, (step 10), ... to #1010 were analyzed. An additional noise filter was added to help with the analysis. Figure 1 shows the original image of Slice #0520 with ROI placed on the four cooling holes of A, B, C, & D. Figure 2 - the 7x magnification of ROI on the four holes 'after' enhancement.

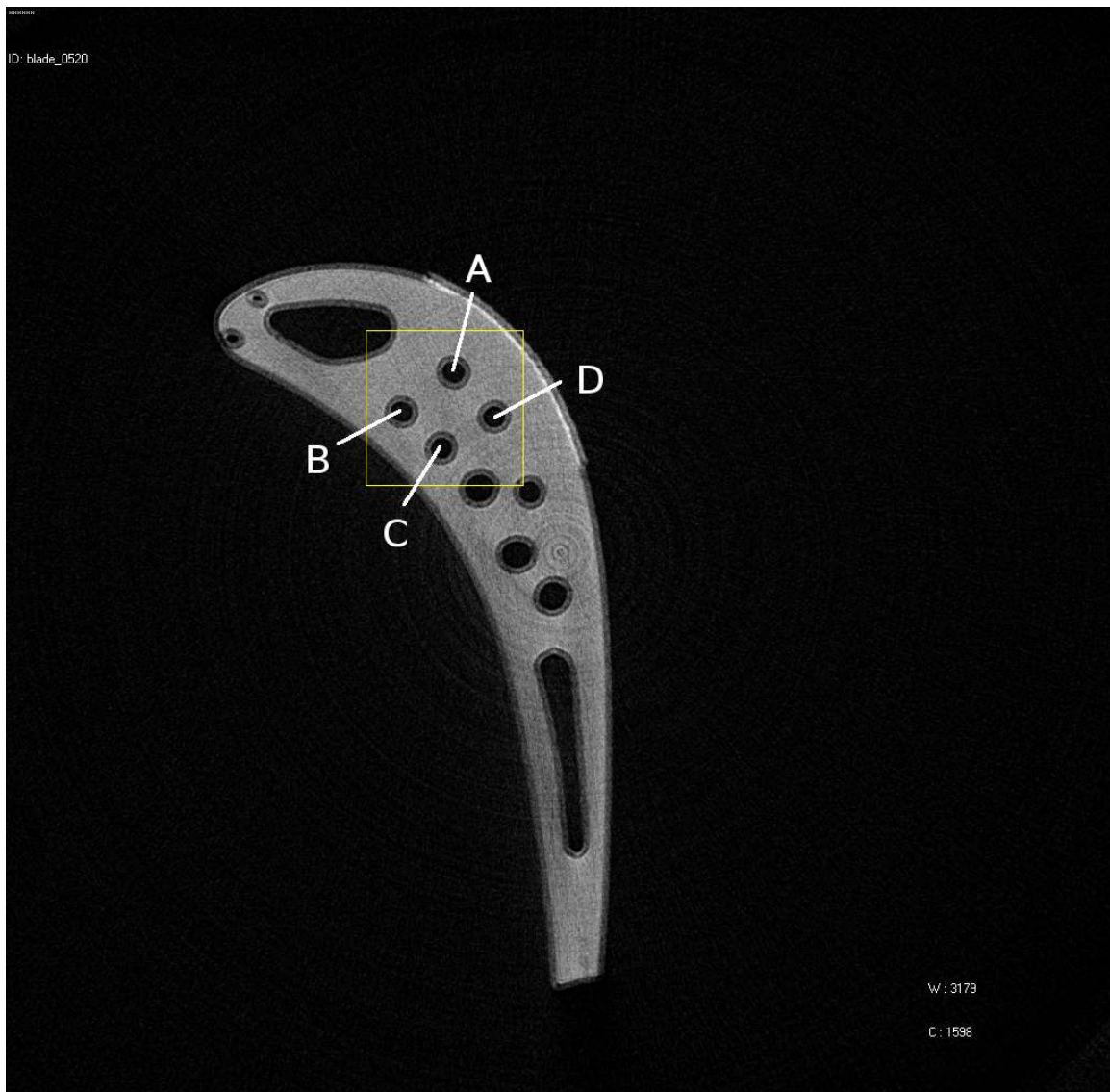


Figure 1 shows the original image of Slice #0520 with ROI placed on the four cooling holes A, B, C, & D.

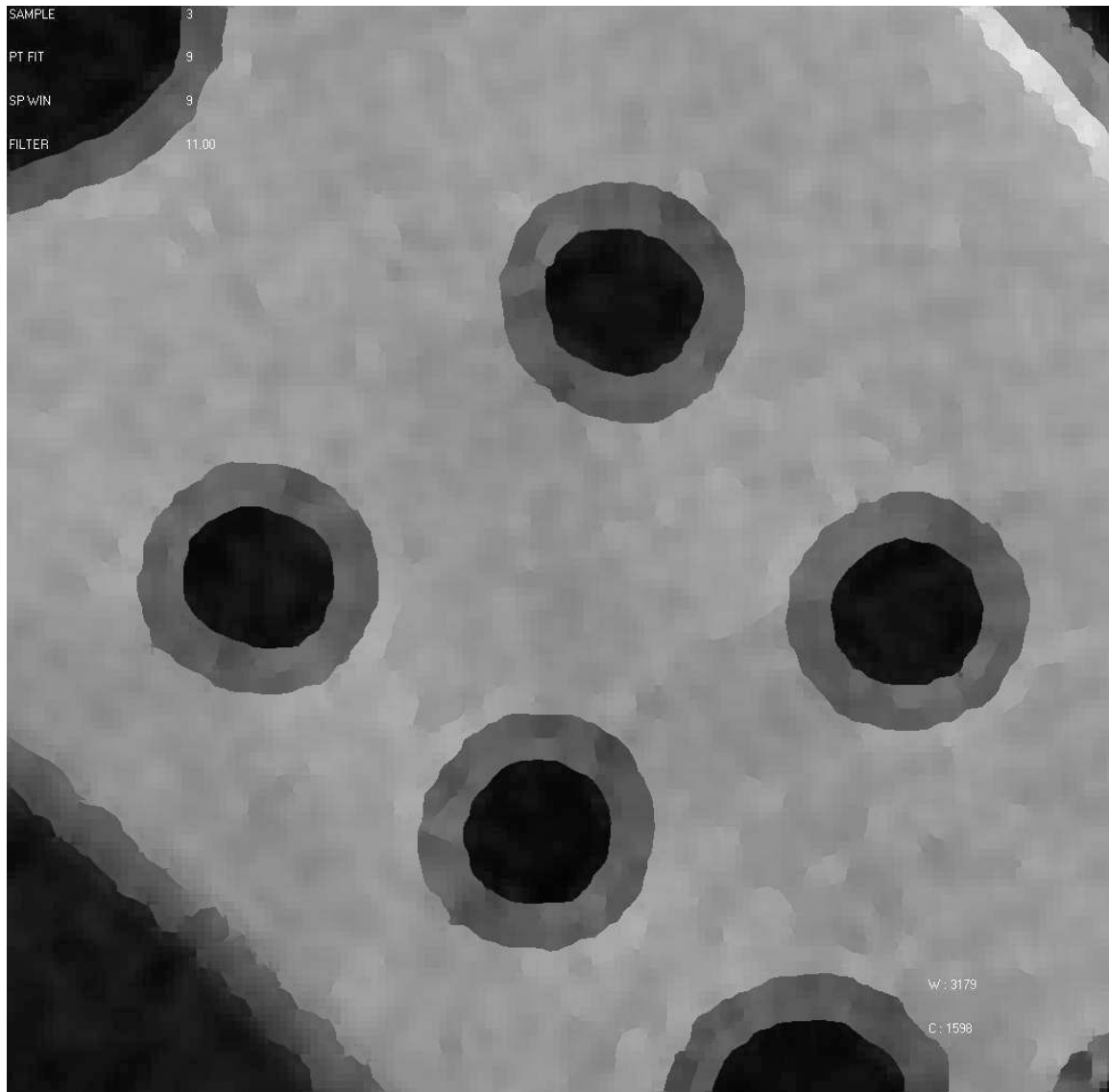


Figure 2 – 7xROI 'after' enhancement on the four cooling holes of Slice#0520

Batch Processing may be used to process a large number of image slices.

We zoomed in on a single hole for a clearer view. Figure 3 shows the original image of Slice#0620 with ROI placed on Hole B. Figure 4 - the 7x ROI 'before' enhancement. Figure 5 – 7x ROI 'after' enhancement. Figure 6 – the enhanced image with annotation for measurement.



Figure 3 – Original image of Slice#0620 with ROI placed on Hole B

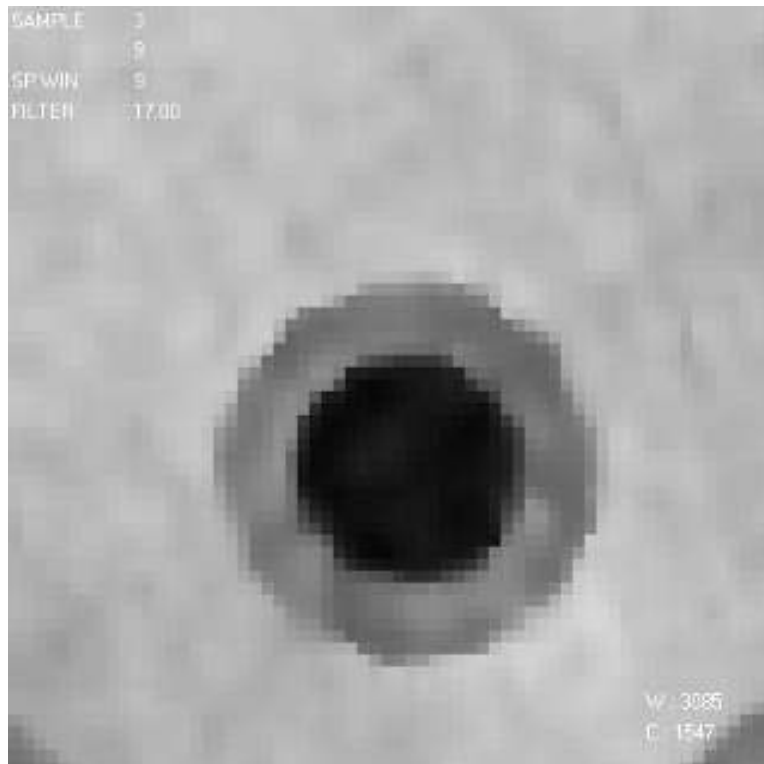


Figure 4 – 7x ROI on Hole B 'before' enhancement.

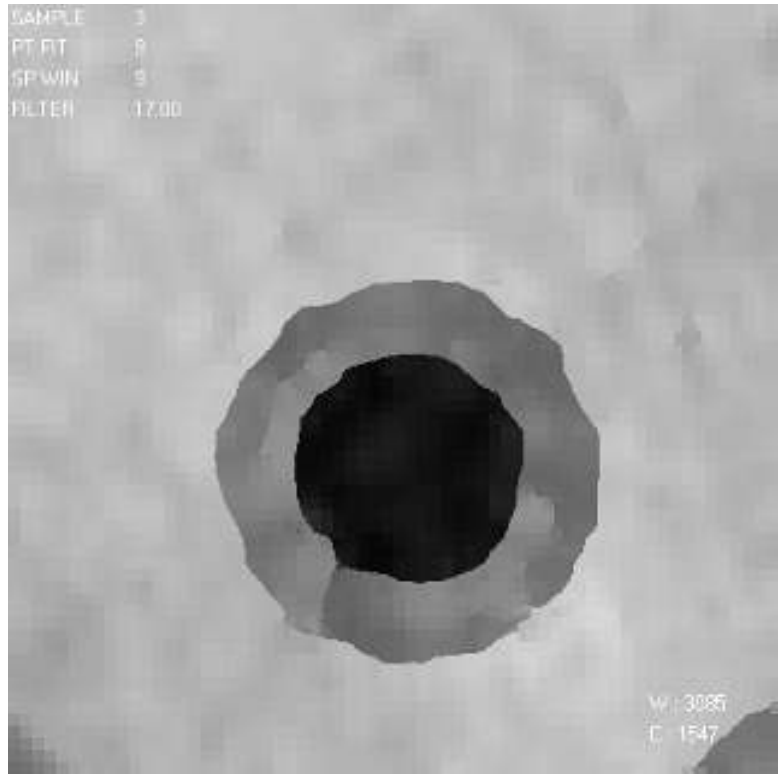


Figure 5 – 7x ROI on Hole B 'after' enhancement.

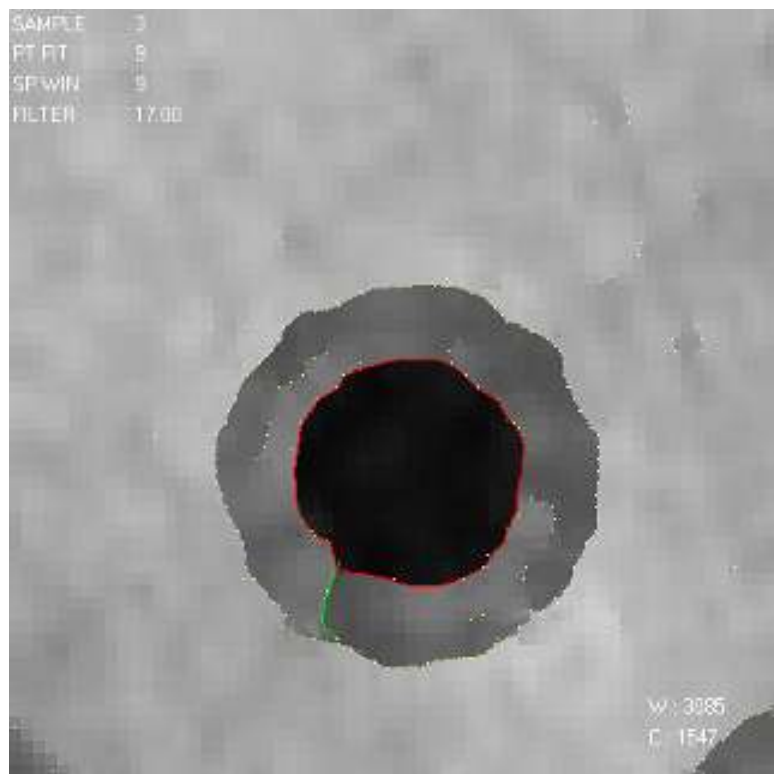


Figure 6 – Enhanced image with edge-profiles & annotations for measurements

Again, batch processing may be used to process a large number of image slices.

The animated views of the enhanced images, first with the region of interest (ROI) placed on the 4 holes, and then zoomed on a single hole set were displayed:

(1) <http://www.iet.org.uk/img/nbct-blade2-animation.gif>

(2) <http://www.iet.org.uk/img/nbct-blade-animation.gif>

Detections: Viewing through the analyzed image sets,

(a) a short fracture was detected at Hole B at Slice #0590, and

(b) a longer hairline fracture was detected at Hole B at Slice #0620

Measurements: Area, A of Hole B at Slice #0620 = 280 pixel² => .049mm².

Length of fracture = 7.16 pixels => .095mm.

(pixel size = .0132mm/pixel)

3. Conclusion

Detection of minute defects and hyper-accurate length measurement of a previously invisible fracture is now possible. The technique may be used for:

(1) Quality control during the original manufacturing process of components.

(2) The monitoring of the condition of in-service components prior to reuse.

4. References

[1]. "A De-Convolution Technique used for NDT in X-ray & CT", by Kui M. Chui, Shyr L.Chui, Andrew Wride, & David B. Stanfield, Oral/Full paper presentation in 17th World Conference on Non-destructive Testing (17WCNDT), Shanghai, China, October 25-28, 2008. (www.ndt.net - The e-Journal & Database of Non-Destructive Testing ISSN 1435-4934).

[2]. "The ICON beamline - A facility for cold neutron imaging at SINQ", by A. Kaestner, S. Hartmann, G. Kuehne, G. Frei, C. Gruenzweig, L. Josic, F. Schmid, E. Lehmann, Nuclear Instruments and Methods in Physics Research Section A: Accelerators, Spectrometers, Detectors and Associated Equipment 659(1), 2011, pp. 387-393.